SCIENTIFIC REPORTS

OPEN

SUBJECT AREAS:
ELECTRONIC STRUCTURE
ELECTRONIC PROPERTIES AND MATERIALS

Received
25 September 2014

Accepted
28 November 2014

Published
16 December 2014

Correspondence and requests for materials should be addressed to G.Q. (qingw@smm.neu.edu.cn)

* These authors contributed equally to this work.

Novel stable hard transparent conductors in TiO_2-TiC system: Design materials from scratch

Xiangying Meng[1,2]*, Dongyan Liu[2], Xuefeng Dai[2], Haijun Pan[1], Xiaohong Wen[1], Liang Zuo[1] & Gaowu Qin[1]*

[1]Key Laboratory for Anisotropy and Texture of Materials (MOE), Northeastern University, Shenyang 110819, China, [2]College of Sciences, Northeastern University, Shenyang 110819, China.

Two new ternary compounds in the TiO_2-TiC system, $Ti_5C_2O_6$ and $Ti_3C_2O_2$, are reported for the first time based on ab initio evolutionary algorithm. $Ti_5C_2O_6$ has a tube-structure in which sp^1 hybridized carbon chains run through the lattice along the *b*-axis; while in the $Ti_3C_2O_2$ lattice, double TiO_6 polyhedral are separated by the non-coplanar sp^2 hybridized hexagon graphite layers along the *c*-axis, forming a sandwich-like structure. At ambient conditions, the two compounds are found to be mechanically and dynamically stable and intrinsic transparent conductors with high hardness (about twice harder than the conventional transparent conducting oxides). These mechanical, electronic, and optical properties make $Ti_5C_2O_6$ and $Ti_3C_2O_2$ ternary compounds be promising robust, hard, transparent, and conductive materials.

Transparent conductive materials (TCMs) play important roles in information and energy technologies, and are widely used in the fields such as photovoltaic devices, sensors, flat-panel displays, and organic light-emitting diodes[1]. Traditional TCMs are based on metals or semiconductors. Metals, for example Al, Ag, and Cu, have good conductivities, but their high electron concentrations[2] ($> 5 \times 10^{22}$ cm^{-3}) bring metals' plasmon energies into the deep-ultraviolet spectral range, thus endowing them with a high absorption in the visible spectral range. Of the different semiconductors available, typically SnO_2, ZnO and In_2O_3 gained widespread attention for their potential applications in the visible and near-ultraviolet spectral range. To make them conductive, element doping was adopted and SnO_2:X, In_2O_3:Sn (ITO) and ZnO:X (where 'X' is a dopant) become popular transparent conductive oxides (TCOs) today. However, an intrinsic conductor with a good transmittance at the visible region is an ideal target in view of conductive and optical requirements, especially in the field of solar energy.

Although be paid less attentions, the mechanical parameters also have direct implications for the high performance of TCM-based devices or designing stress-free TCM films on both rigid and flexible substrates. The studies on the mechanical properties so far have been mainly on the scratch resistance of TCM films. Not much is known about the design principles on the hard transparent conductors. One guiding suggestion for forming hard materials has been to increase the sp^3 concentration in which tetrahedral hybrids contributes to the hardness, and extensive experimental and theoretical efforts have been devoted to searching of diamond-like covalent compounds formed by B, C, and N[3–5]. However, those sp^3-bonded materials are often related to a wide band gap, and there is no reason to expect these compounds comparable in hardness to diamond would show conductivity. On the contrary, the conventional TCOs, such as F-doped SnO_2 (FTO), Zn-doped In_2O_3 (IZO), and ITO, have a Vickers hardness lower than 10 GPa[6,7], thus the contradictory mechanical and electrical properties seem hardly to coexist in a stable compound.

An inspiration for designing hard transparent conductors can be derived from graphene[8,9]. This hard carbon film is a zero bandgap semiconductor with a low resistivity comparable to metals ($\sim 10^{-8}$ Ωm) and low high electron concentrations ($< 0.3 \times 10^{21}$ cm^{-3}) endowing it almost fully transparent at visible region[2]. At present, the development of graphene as a TCM is largely restricted by the coupling between graphite sheets. Since the outstanding mechanical, electronic and optical properties of graphene are attributed to the hybrids of sp^2 bonds formed intra-graphite sheet, it is expected to fabricate a sandwich-like structure in which the sp^2 bonded graphite layers is clipped through hybridized bonding by two "buns". The strong hybrids between sheets keep the hardness,

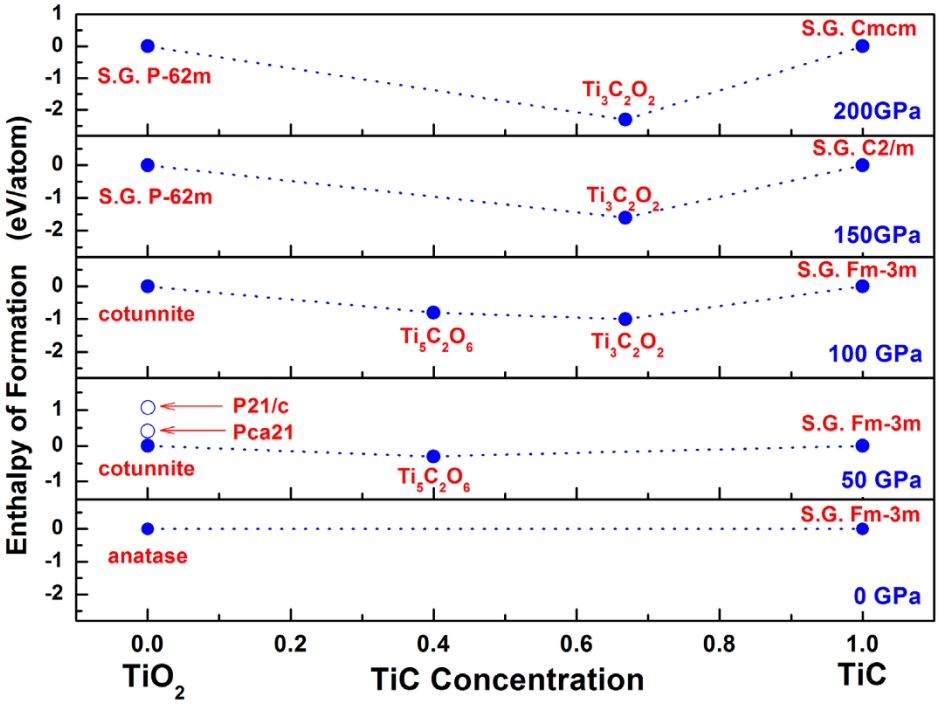

Figure 1 | Thermodynamical stability of novel Ti-C-O ternary compounds. Convex hull diagram for the TiO_2-TiC system at selected pressures. The blue solid circles represent stable compounds, and the open circles represent meta-stable compounds.

and the sp^2 bonds in the graphite layer promote conductivity. In addition, this structure should be thermodynamically, mechanically, and dynamically stable at ambient conditions.

In order to explore a compound meeting those stringent conditions, we need to select an appropriate system in which the desirable performances may be obtained. Many experimental and theoretical studies indicate that TiO_2 have a series of high-pressure phases possessing very high hardness. For example, the cotunnite-structured TiO_2 was once thought to be the hardest oxide[10], and the Fe_2P-type TiO_2 was proved to be the densest phase in major metal dioxides[11]. In addition, doped-TiO_2 was reported to be a transparent oxide[12]. Thus the hardness and transparency requirements can be expected in the TiO_2-based system. To pursue high conductivity, we should further introduce carbon element and TiC is thus chosen as the other terminal compound which has a comparable bulk moduli (241 GPa)[13] to that of the cotunnite-structured TiO_2 (246 GPa)[11]. Therefore, the TiO_2-TiC pseudo-binary system is a promising candidate in which our desired mechanical, electrical and optical properties may be achieved through a stable Ti-C-O ternary compound. However, such a ternary compound is not available at ambient conditions according to the present phase diagram and crystal structure database.

The high-pressure behavior of materials now can be experimentally studied at pressures over 300 GPa[14], which motivates searching high-pressure phases in various systems by ab-initio simulations[15,16]. In the present work, thermodynamically stable compounds in TiO_2-TiC system are searched at both ambient and selected high pressures using evolutionary algorithm USPEX[17–20]. This popular method is reasonable and accurate in the multidimensional-compounds-predicting and can simultaneously search stable stoichiometries and the corresponding structures together in multi-component systems. Furthermore, the properties of observed novel intermediate compounds in the TiO_2-TiC system, including mechanical modulus, electronic structure, and optical absorption, are investigated to test our tentative ideals. For the first time, we report two Ti-C-O ternary hard and transparent conductors, namely $Ti_5C_2O_6$ and $Ti_3C_2O_2$. Both compounds are stable at ambient conditions with wonderful structural, mechanical, electronic, and optical properties.

Results and Discussion

The detail convex hull diagram of TiO_2-TiC system at selected pressures are shown in Fig. 1, and we will discuss structural, mechanical, electronic, and optical properties of stable compounds in the following two sections.

Terminal compounds in TiO_2-TiC system. In TiO_2 family, many phases[11,21] at constant-, low-, or high-pressure conditions have been reported including anatase (AN), rutile (RT), brookite (BR), columbite (CB), baddeleyite (MI), orthorhombic I (OI), pyrite (PI), fluorite (FL), cotunnite (OII), and Fe_2P-TiO_2.

In most studies, the starting material at ambient pressure is AN or RT. AN is believed to be more stable than RT when the particle size decreases below 14 nm[22]. CB and MI are low-pressure phases (below 20 GPa) and the transition sequence under pressure are AN or RT or BR→CB→MI[21]. At 35 GPa, a P*ca21*-TiO_2 is found energetically close to the MI and cotunnite, and conceived as a metastable polymorph of TiO_2[23]. Above 50 GPa, OI, PI, and FL phases were experimentally and theoretically reported to convert to the OII phase[10,21], suggesting that the cotunnite becomes more stable after overcoming a energy barrier. Above 150 GPa, as a post-cotunnite phase, the existence of Fe_2P-TiO_2 has been proved by a recent crucial high-pressure experiment[11].

According to Fig. 1, the enthalpy searching algorithm implemented in USPEX yields anatase-TiO_2 (space group *I41/amd*) and cotunnite-TiO_2 (space group *Pnma*) as the final thermodynamically stable phases at ambient and selected high pressure range (50 ~ 150 GPa), respectively. At 50 GPa, we further analyzed the metastable phases relative to the stable cotunnite. The closest structure in energy to the cotunnite is P*ca21*-TiO_2, then baddeleyite-TiO_2 (space group *P21/c*) is found as a next-metastable phase. The calculated energetic order is consistent with the reported pressure-induced phase transition of TiO_2 around 50 GPa[24]. Above 150 GPa, USPEX finds that the Fe_2P-TiO_2 (space group *P-62m*) high-pressure phase become more stable. Thus, our present theoretical predictions on the stable phases of TiO_2 at different pressures are well consistent with the known experi-

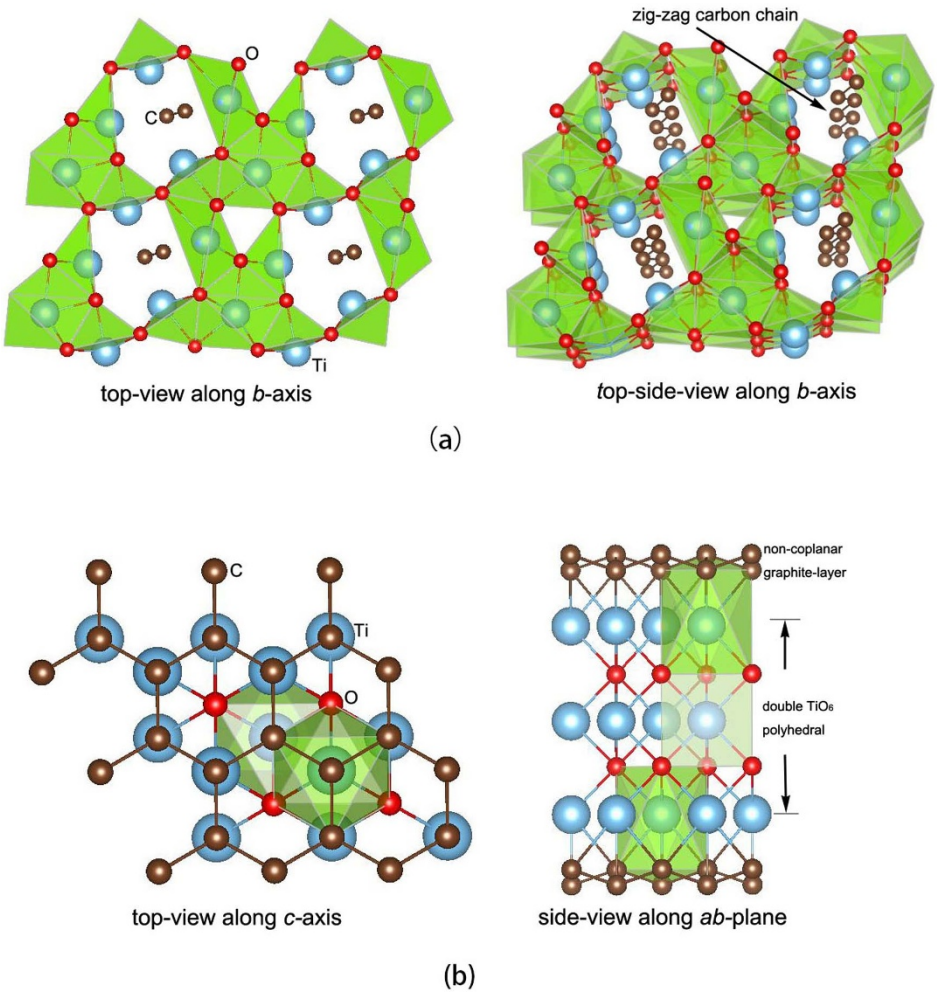

Figure 2 | Structural feature. Top- and side- views of $Ti_5C_2O_6$ (a) and $Ti_3C_2O_2$ (b) lattices. In $Ti_5C_2O_6$, the zigzag carbon chains run through Ti-O polyhedral along the *b*-axis. In $Ti_3C_2O_2$, TiO_6 polyhedral are separated by the non-coplanar hexagon graphite layers along the *c*-axis. In (a) and (b), cyan atoms represent titanium, brown atoms represent carbon, and red atoms represent oxygen.

mental observations, further confirming that USPEX predictions are reasonable.

The other terminal, TiC, was found as a NaCl-B1 (space group *Fm-3m*) structured crystal at ambient conditions[25]. In Fig. 1, our detailed enthalpy calculations show that B1-structured TiC seems unshakeable until ~100 GPa. Then *C2/m*-TiC is found more thermodynamically stable between 100 ~ 150 GPa. Finally, *Cmcm*-structure notably appeared above 150 GPa as the final high-pressure phase for TiC.

Several transition mechanisms have been used to interpret the high pressure phase transition of B1-structured carbides. It was proposed that most B1-structured compounds follow the B1→CsCl-B2 phase transition route under pressure[26]. Then, it was experimentally reported that a B1→R (rhombohedron), instead of B1→B2, phase transition in TiC occurred at a pressure above 18 GPa[27]. However, after re-evaluating these experiments, no phase transition in TiC was really found at pressures up to 26 GPa[28]. Recently, a new B1→*C2/m*→*Cmcm* three high-pressure phase transition route for TiC was put foward[29]. Our predictions on TiC high-pressure phases totally support this latest investigation.

Novel intermediate compounds in TiO_2-TiC system. Based on the convincing results above related to TiO_2 and TiC terminal compounds, we can further predict Ti-C-O ternary stable phases in the TiO_2-TiC system. In Fig. 1, no thermodynamically stable Ti-C-O ternary compound is observed at 0 GPa. This is consistent with the currently known inorganic crystal structure data. Then, as the first stable intermediate compound in the TiO_2-TiC system, $Ti_5C_2O_6$ (TiO_2:TiC=3:2) appears at ~50 GPa with a monoclinic structure (space group *Pm*). At a higher pressure (~100 GPa), the second intermediate compound $Ti_3C_2O_2$ (TiO_2:TiC=1:2) with a hexagonal lattice (space group *P3m1*), is further found thermodynamically stable in the TiO_2-TiC system. Detailed enthalpy calculations show that *Pm*-$Ti_5C_2O_6$ phase disappears at ~130 GPa, while *P3m1*-$Ti_3C_2O_2$ phase can be thermodynamically stable up to 200 GPa in the TiO_2-TiC system.

$Ti_5C_2O_6$ and $Ti_3C_2O_2$ has respective unique structural feature. In the $Ti_5C_2O_6$ lattice, the sp^1 hybridized zigzag carbon chains are surrounded by Ti-O polyhedral and run through these cages along the *b*-axis, forming a tube-structure; while in the $Ti_3C_2O_2$ lattice, double TiO_6 polyhedral are separated by the sp^2 hybridized non-coplanar hexagon graphite layer along the *c*-axis, forming a sandwich-like layer structure. The detail top and side views of the two structures are presented in Fig. 2. The full structural parameters (in *cif* format) of two compounds can be found in the Supplementary Information.

To check the dynamical stability at ambient conditions for the two new Ti-C-O ternary compounds, their structures are fully relaxed and phonon dispersion curves at 0 GPa are calculated. In Fig. 3, no imaginary phonon frequency is observed in the whole Brillouin-zone, indicating that $Ti_5C_2O_6$ and $Ti_3C_2O_2$ are both dynamically stable at ambient pressure.

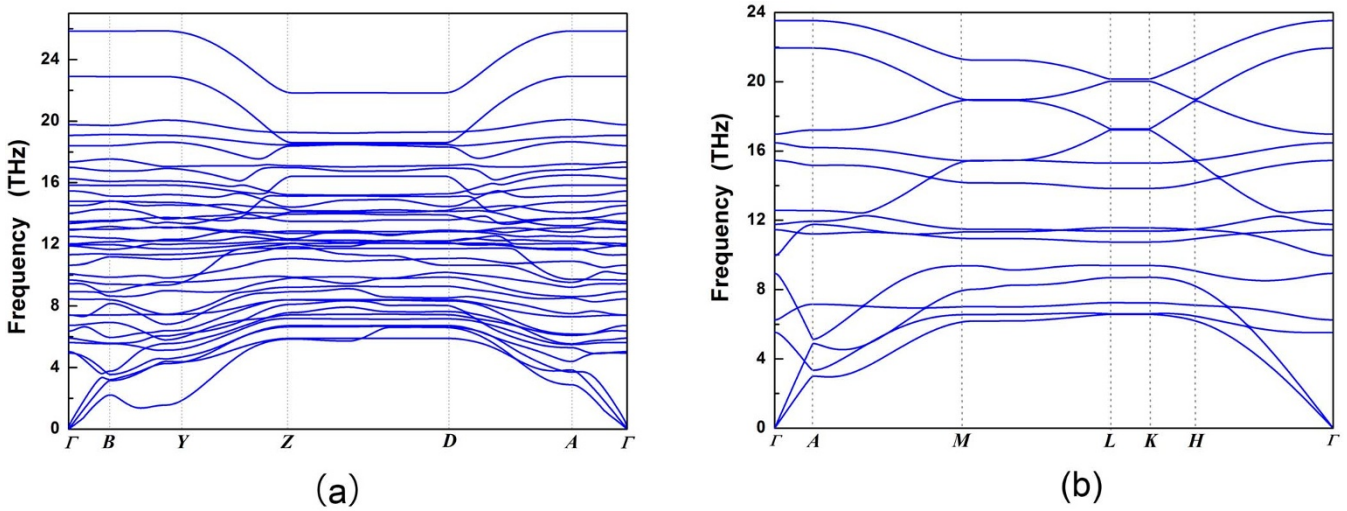

Figure 3 | **Dynamical stabilities.** Phonon dispersion curves at 0 GPa for $Ti_5C_2O_6$ (a) and $Ti_3C_2O_2$ (b). No Imaginary frequency is observed in the whole Brillouin-zone.

The mechanical stability of a structure can be assessed by the elastic constants of the crystal which should satisfy Born elastic stability criteria. Using stress-strain relations, the independent elastic constants of $Ti_5C_2O_6$ and $Ti_3C_2O_2$ phases at the zero-pressure are calculated and listed in the Supplementary Information (Table Is). For the monoclinic-$Ti_5C_2O_6$, the mechanical stability[30] are indicated by $C_{11} > 0, C_{22} > 0, C_{33} > 0, C_{44} > 0, C_{55} > 0, C_{66} > 0, [C_{11} + C_{22} + C_{33} + 2(C_{12} + C_{13} + C_{23})] > 0, (C_{33}C_{55} - C^2_{35}) > 0, (C_{44}C_{66} - C^2_{46}) > 0$ and $(C_{22} + C_{33} - 2C_{23}) > 0$; while the stability criteria[30] for the hexagonal-$Ti_3C_2O_2$ are given by $C_{44} > 0$, $C_{11} > |C_{12}|$ and $(C_{11} + 2C_{12})C_{33} > 2C^2_{13}$. Obviously, the calculated elastic constants of two ternary compounds fulfill their respective stability criteria.

It is believed the hardness of a compound are related to the elastic parameters, namely bulk modulus B, shear modulus G, Young's modulus E, and Poisson's ratio v[31]. B and G are calculated by means of the single-crystal elastic constants and the Voigt-Reuss-Hill relations[32], and E and v can be subsequently deduced as $E = 9BG/(3B + G)$ and $v = (3B - 2G)/[2(3B + G)]$, respectively. In Table I, the calculated bulk moduli for $Ti_5C_2O_6$ and $Ti_3C_2O_2$ (228 GPa and 259 GPa) are close to that of cotunnite-TiO_2 (246 GPa)[10]. It was believed that materials having lower G/B and higher v will exhibit better intrinsic plasticity[33], and we can thus predict that $Ti_5C_2O_6$ has a more flexible lattice while the structure of $Ti_3C_2O_2$ is relatively rigid.

The hardness of a crystal can be directly rated by Vickers hardness (H_V). The macro- and micro-models for the hardness prediction can be found in Tian's report[34]. In this study, we evaluate H_V of two ternary Ti-C-O compounds based on both Chen's macro-fitting formula[35,36] and the micro-electronegativity (EN) model[37,38]. Using Chen's formula:

$$H = 0.92(G/B)^{1.137}G^{0.708} \quad (1)$$

Table I | The bulk modulus B, shear modulus G, Young's modulus E, Poisson's ratio v, and G/B ratio of monoclinic-$Ti_5C_2O_6$ and hexagonal-$Ti_3C_2O_2$. All elastic parameters except v and G/B are in GPa

	B	G	E	v	G/B
$Ti_5C_2O_6$	228	135	338	0.25	0.59
$Ti_3C_2O_2$	259	173	424	0.23	0.67

the hardness of a compound can be directly obtained from its bulk and shear modulus. For a covalent crystal with n-types of bonds, micro-EN hardness is expressed as

$$H(GPa) = \frac{423.8}{V}\left[\prod_{a,b=1}^{n} N_{ab}X_{ab}e^{-2.7f_i(ab)}\right]^{1/n} - 3.4 \quad (2)$$

where V is the volume of the unit cell (Å^3) and N_{ab} is the number of bonds of a-b kind in the unit cell. Coefficients 423.8, 2.7, and −3.4 were obtained in Ref. 37 by fitting to experimental data for hard materials. In the equation (2), f_i is an ionicity indicator of the band a-b, and X_{ab} is named as the bond-EN between atoms a and b. In the EN model, f_i and X_{ab} can be deduced from the element-EN and element coordination number (CN) in the form of

$$f_i = \frac{|\chi_a - \chi_b|}{4\sqrt{\chi_a\chi_b}}; \quad (3)$$

$$X_{ab} = \sqrt{\frac{\chi_a\chi_b}{CN_aCN_b}} \quad (4)$$

where χ_a and χ_b are the EN of elements a and b, and CN_a and CN_b are respective coordination number of atoms a and b. In $Ti_5C_2O_6$ and $Ti_3C_2O_2$, three types of bands, *i.e.* Ti-O, Ti-C, and C-C, are formed. The detail parameters are listed in Table II, and both macroscopic and microscopic models yields consistent hardness: ~16 GPa and ~22 GPa for $Ti_5C_2O_6$ and $Ti_3C_2O_2$, respectively. It was reported that the experimental hardness of ITO and IZO is 6.5 ± 1.6 GPa and 10.6 ± 3.3 GPa[39], respectively, thus we surprisingly found that the two new T-C-O compounds are about twice harder than these conventional transparent conducting oxides.

Table II | The Vickers hardness (in GPa) of monoclinic-$Ti_5C_2O_6$ and hexagonal-$Ti_3C_2O_2$. H_{mic} is the hardness calculated with the micro-electronegativity (EN) model, while H_{mac} is obtained through the macro-fitting formula

	A-N	$\chi_{A\text{-}N}$	f_i	V(Å^3)	H_{mic}	H_{mac}
$Ti_5C_2O_6$	Ti-C	0.169	0.136	101.66	16.95	16.34
	Ti-O	0.187	0.260			
	C-C	0.357	0.000			
$Ti_3C_2O_2$	Ti-C	0.273	0.136	50.08	23.29	22.30
	Ti-O	0.384	0.260			
	C-C	0.357	0.000			

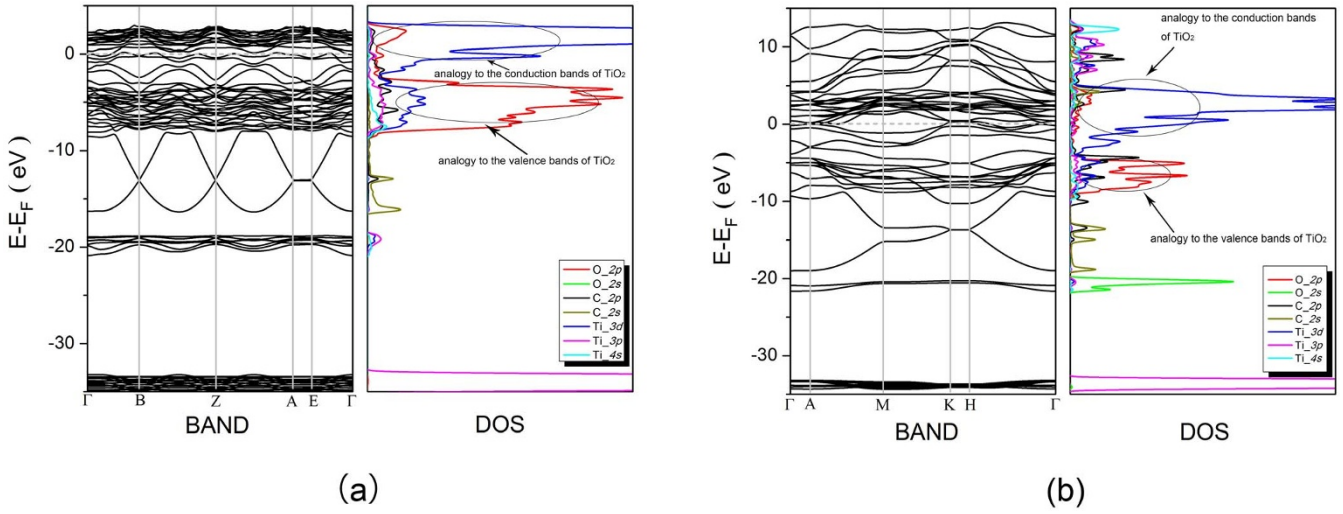

Figure 4 | Electronic properties. Band structures and partial density of electronic states (PDOSs) at 0 GPa for $Ti_5C_2O_6$ (a) and $Ti_3C_2O_2$ (b), which show the metallic properties of two novel ternary compounds. Bonding features that are similar to the valence bands and conduction bands in anatase-TiO_2 are circled by the ovals.

The PBE[40] exchange-correlation functional is used to calculate the band structures and partial density of electronic states (PDOS) of $Ti_5C_2O_6$ and $Ti_3C_2O_2$. In Fig. 4, electronic structure calculations clearly show that $Ti_5C_2O_6$ and $Ti_3C_2O_2$ are intrinsic conductors. By comparison, the band structures of two new ternary compounds obtained by the HSE[41] method are shown in the Supplementary Information and no bandgaps are found, which further proves the metallic properties of two compounds. We compare PDOS of $Ti_5C_2O_6$ and $Ti_3C_2O_2$ with that of TiO_2. For TiO_2 semiconductor, it was known that its upper valence band is essentially of O-2*p* bonding type with a small presence of Ti-3*d* states, and the edge of conduction band is dominated by Ti-3*d* orbitals with a small contribution from O-2*p* levels[42]. In the $Ti_5C_2O_6$ and $Ti_3C_2O_2$ ternary compounds, we found similar bonding feature analogy to the valence bands and conduction bands in TiO_2 (see Fig. 4). However, the original band gaps in TiO_2 are filled by Ti-C bonds in the Ti-C-O compounds in which Fermi-levels are located at the conduction bands zone. Therefore, $Ti_5C_2O_6$ and $Ti_3C_2O_2$ are proposed as electron (*n*-type) conductors.

From the PDOS, the contribution of carbon atoms to the density of states at Fermi level is much smaller than the *3d* state of Ti atoms. To understand the conductive properties of novel compounds, we further calculated the conductivity components σ_{ij}/τ (3×3 tensor) of $Ti_3C_2O_2$ based on Boltzmann transport theory[43], where τ is the electron relaxation times and is a constant in the compound (See details in the Supplementary Information). The results suggest that the conductivity of $Ti_3C_2O_2$ is significantly anisotropic, and the conductivity components along the *a* or *b* axis is about 10 times higher than that along the *c* axis. In $Ti_3C_2O_2$, the TiO part is stacked along the *c* axis while carbon is extended along the *ab* plane. Then we can deduce that the TiO part contribute little to the conductivity when compared with carbon. A major channel for the carrier transport may be expressed as that the nonlocalized Ti_*3d* electrons move to carbon through the Ti-C coupling, and then flow along *ab* plane through the graphite layers. The $Ti_5C_2O_6$ compound may hold similar hypothesis.

The stable, hard, and conductive characteristics of these two ternary compounds drive us to further investigate their transparency towards visible light band. The calculated optical absorption coefficients of $Ti_5C_2O_6$ and $Ti_3C_2O_2$ are shown in Fig. 5 and compared with that of SnO_2, a principal constituent of conventional TCOs. It delights us that $Ti_3C_2O_2$ has a weaker optical absorption activity than SnO_2 in the visible light region, indicating that $Ti_3C_2O_2$ is more transparent. However, $Ti_5C_2O_6$ is not as good as $Ti_3C_2O_2$ at the optical transparency in view of its relative higher optical absorption than SnO_2. The optical absorption coefficient is frequency dependant, and different optical adsorption behaviors of $Ti_3C_2O_2$ and $Ti_5C_2O_6$ are related to their respective electronic transitions between energy levels.

The primary *n*-type TCOs have remained virtually unchanged for about 30 years. FTO, ITO, and F- or Al-doped ZnO[44] have been the principal commercial TCOs[45]. Recent work has begun to explore ternary compounds, for example Cd_2SnO_4, Zn_2SnO_4, $MgIn_2O_4$, $ZnSnO_3$, $GaInO_3$, $Zn_2In_2O_5$, and $ZnGa_2O_4$, as new *n*-type transparent conductive materials[46–50]. Our novel Ti-C-O ternary compounds in the TiO_2-TiC system, $Ti_5C_2O_6$ and $Ti_3C_2O_2$, are found to have attractive mechanical, electronic, and optical properties, and can be more robust, cost-effective and environmentally benign TCOs used in the environments where conventional transparent conducting materials have difficulties. Following the same materials designing route, we propose that Zr(Hf)O_2-Zr(Hf)C can also be expected as promising pseudo-binary systems in which wonderful TCOs may exist, because Zr(Hf)O_2 and Zr(Hf)C are similar to TiO_2 and TiC in the aspects of structure and phase transition characteristics. The ideals and schemes adopted here toward searching and designing multi-components materials is instructive for developing novel functional materials in the near future.

In summary, to develop novel hard transparent conductors, we explore Ti-C-O ternary compounds in the TiO_2-TiC system at ambient and selected high-pressure conditions using ab-initio evolutionary algorithm USPEX. Two new compounds, $Ti_5C_2O_6$ and $Ti_3C_2O_2$, are reported for the first time and found to be mechanically and dynamically stable at the ambient pressure with respective unique structure. The sp^1 hybridized carbon chains and sp^2 hybridized hexagon graphite layers enable $Ti_5C_2O_6$ and $Ti_3C_2O_2$ to be efficient intrinsic conductors, while the high-coordinated Ti-O polyhedral guarantee their hardness to be twice harder than that of conventional transparent conducting materials. The optical transparencies of two new compounds are comparable to that of SnO_2 in the visible light band and $Ti_3C_2O_2$ is more transparent. These mechanical, electronic, and optical properties make $Ti_5C_2O_6$ and $Ti_3C_2O_2$ be attractive hard transparent conductors. More significantly, the ideals and methods towards designing and predicting materials in this work can be applied to other compound systems for the searching of novel functional materials.

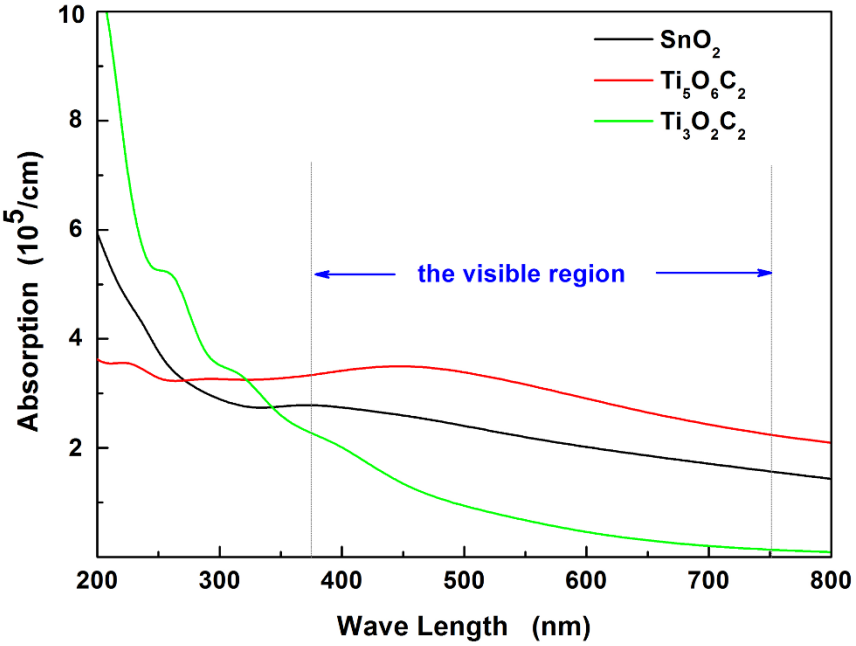

Figure 5 | Optical absorptions. The absorbance of $Ti_5C_2O_6$ and $Ti_3C_2O_2$ compared with that of SnO_2 bulk materials. In the visible region, the lower optical absorption in $Ti_3C_2O_2$ results in an increased transparency relative to SnO_2.

Methods

USPEX structure prediction. Combining the evolutionary algorithm USPEX[17–20] with the ab-initio total energy program VASP[51], we predict thermodynamically stable structures in the TiO_2-TiC system. To construct the pseudopotentials (PPs) of Ti, C, O elements, we treat their respective $3s^23p^64s^23d^2$, $2s^22p^2$, and $2s^22p^4$ orbitals as valence electronic configurations throughout this work. For bulk geometry optimizations, PBE[40] exchange-correlation functional with and without the van der Waals correction[52] are adopted respectively and two functionals lead to same results. The plane-wave kinetic energy cutoff is set to 600 eV, and the Brillouin zone is sampled with a resolution of $2\pi \times 0.05$, which show excellent convergence of the energy differences, stress tensors and structural parameters. The maximum total numbers of atoms in the unit cell are limited to 16 and 32, respectively, and enthalpy calculations are performed at pressures of 0 GPa, 50 GPa, 100 GPa, 150 GPa, 200 GPa. The first generation of structures is created randomly, then energetically worst structures (40%) are discarded and a new generation is created from the remaining structures through heredity, lattice mutation and permutation of atoms. The most favorable structures are transferred into the next generation. We generally terminate the runs after 50 generations, and all runs have found the minimum-enthalpy structures much earlier.

Phonon dispersion curves. All obtained intermediate compounds are fully relax at constant pressure. To ensure sufficient convergence criteria, the total Hellmann-Feynman force with respect to the structural degrees of freedom is set to 0.01 meV/Å. The quasi-harmonic approximation which has been implemented in the PHON code[53] is used to calculate phonon dispersion curves.

Electronic and optical properties. The electronic calculations for the stable Ti-C-O conductors are performed based on density functional theory (DFT) within the framework of PBE approximation. The kinetic-energy cutoff for electronic plane waves is set to 600 eV and the Brillouin-zone integrations are performed using $18 \times 18 \times 18$ k-point meshes. The optical absorptions are calculated using HSE[41] functional which has been implemented in the VASP code. The frequency dependent dielectric matrix are first determined based on the calculations of electronic ground states, then the absorption coefficients can be derived from the real and imaginary parts of the dielectric function[54].

Ideal shear strength. The shear stress is calculated by straining the crystal in a series of incremental simple shears, calculating the stress as a function of the strain[55]. Here, a series of shear strains perpendicular to the carbon chains and to the normal of graphite planes are applied to $Ti_5C_2O_6$ and $Ti_3C_2O_2$ equilibrium cell, respectively. Using a Cartesian coordinate, the x-vector is selected as perpendicular to the slip plane and the z-vector parallel to the slip direction in the plane. Incrementally deformed lattices are relaxed with respect to the basis vectors orthogonal to the applied strain and the atoms inside the cell.

1. Ginley, D. S., Hosono, H. & Paine, D. C. *Handbook of Transparent Conductors* (Springer, 2010).
2. Ellmer, K. Past achievements and future challenges in the developments of optically transparent electrodes. *Nat. Photonics* **6**, 809–817 (2012).
3. Liu, A. Y. & Cohen, M. L. Prediction of new low compressibility solids. *Science* **245**, 841–842 (1989).
4. Cohen, M. L. Predicting useful materials. *Science* **261**, 307–308 (1993).
5. Tian, Y. *et al.* Ultrahard nanotwinned cubic *Boron nitride*. *Nature* **493**, 385–388 (2013).
6. Gao, F. *et al.* Hardness of covalent crystals. *Phys. Rev. Lett.* **91**, 015502 (2003).
7. Gordon, R. G. Criteria for choosing transparent conductors. *Mat. Res. Sci. Bull.* **25**, 52–57 (2000).
8. Hirono, S. *et al.* Superhard conductive *Carbon* nanocrystallite films. *Appl. Phys. Lett.* **80**, 425–427 (2002).
9. Jung, H. Y. *et al.* Transparent, flexible supercapacitors from nano-engineered *Carbon* films. *Sci. Rep.* **2**, 773 (2012).
10. Dubrovinsky, L. S. *et al.* Materials science: The hardest known oxide. *Nature* **410**, 653–654 (2001).
11. Dekura, H. *et al.* Theoretical and experimental evidence for a new post-cotunnite phase of *Titanium dioxide* with significant optical absorption. *Phys. Rev. Lett.* **107**, 045701 (2011).
12. Furubayashi, Y. *et al.* A transparent metal: Nb-doped anatase *TiO_2*. *Appl. Phys. Lett.* **86**, 252101 (2005).
13. Teter, D. M. Computational alchemy: the search for new superhard materials. *Mat. Res. Sci. Bull.* **23**, 22–27 (1998).
14. Sakai, T. *et al.* Equation of state of the *NaCl-B2* phase up to 304 GPa. *J. Appl. Phys.* **109**, 084912 (2011).
15. Zhang, W. *et al.* Unexpected stable stoichiometries of *Sodium chlorides*. *Science* **342**, 1502–1505 (2013).
16. Zhu, Q. *et al.* Stability of xenon oxides at high pressures. *Nat. Chem.* **5**, 61–65 (2013).
17. Oganov, A. R. & Glass, C. W. Crystal structure prediction using *ab initio* evolutionary techniques: Principles and applications. *J. Chem. Phys.* **124**, 244704 (2006).
18. Oganov, A. R. *et al.* Evolutionary crystal structure prediction as a method for the discovery of minerals and materials. *Rev. Mineral. Geochem.* **71**, 271–298 (2010).
19. Oganov, A. R., Stokes, H. & Valle, M. How evolutionary crystal structure prediction works and why. *Acc. Chem. Res.* **44**, 227–237 (2011).
20. Lyakhov, A. O. *et al.* New developments in evolutionary structure prediction algorithm USPEX. *Comp. Phys. Comm.* **184**, 1172–1182 (2013).
21. Khatatbeh, Y. A., Lee, K. K. M. & Kiefer, B. High-pressure behavior of *TiO_2* as determined by experiment and theory. *Phys. Rev. B* **79**, 134114 (2009).
22. Zhang, H. & Banfield, J. F. Thermodynamic analysis of phase stability of nanocrystalline *Titania*. *J. Mater. Chem.* **8**, 2073–2076 (1998).
23. Zhou, X. F. *et al.* Unusual compression behavior of TiO_2 polymorphs from first principles. *Phys. Rev. B* **82**, 060102 (2010).
24. Fu, Z. *et al.* Structural phase transition and mechanical properties of TiO_2 under high pressure. *Phys. Status Solidi B* **250**, 2206–2214 (2013); Dubrovinskaia, N. A. *et al.* Experimental and theoretical identification of a new high-pressure *TiO_2* polymorph. *Phys. Rev. Lett.* **87**, 275501 (2001).

25. Elliott, R. O. & Kempter, C. P. Thermal expansion of some transition metal carbides. *J. Phys. Chem.* **62**, 630–631 (1958).
26. Cohen, A. J. & Gordon, R. G. Theory of the lattice energy, equilibrium structure, elastic constants, and pressure-induced phase transitions in *Alkali-halide* crystals. *Phys. Rev. B* **12**, 3228–3241 (1975).
27. Dubrovinskaia, N. A. *et al*. High-pressure study of *Titanium carbide. J. Alloys Compd.* **289**, 24–27 (1999).
28. Winkler, B. *et al.* Reaction of *Titanium* with *Carbon* in a laser heated diamond anvil cell and reevaluation of a proposed pressure-induced structural phase transition of *TiC. J. Alloys Compd.* **478**, 392–397 (2009).
29. Zhao, Z. *et al.* Universal phase transitions of *B1-structured* stoichiometric transition metal carbides. *Inorg. Chem.* **50**, 9266–9272 (2011).
30. Wu, Z. J. *et al*. Crystal structures and elastic properties of superhard IrN_2 and IrN_3 from first principles. *Phys. Rev. B* **76**, 054115 (2007).
31. Tian, F. *et al*. Superhard semiconducting C_3N_2 compounds predicted via first-principles calculations. *Phys. Rev. B* **78**, 235431 (2008).
32. Hill, R. The elastic behavior of a crystalline aggregate. *Proc. Phys. Soc. A* **65**, 349–354 (1952).
33. Zhang, L. *et al*. Bulk metallic glasses with large plasticity: Composition design from the structural perspective. *Acta Mater.* **57**, 1154–1164 (2009).
34. Tian,Y., Xu, B. & Zhao, Z. Microscopic theory of hardness and design of novel superhard crystals. *Int. J. Ref. Met. Hard Mater.* **33**, 93–106 (2012).
35. Chen, X. Q. *et al*. Modeling hardness of polycrystalline materials and bulk metallic glasses. *Intermetallics* **19**, 1275–1281 (2011).
36. Chen, X. Q. *et al*. Hardness of T-carbon: Density functional theory calculations. *Phys. Rev. B* **84**, 121405 (2011).
37. Li, K. Y. *et al*. Electronegativity identification of novel superhard materials. *Phys. Rev. Lett.* **100**, 235504 (2008).
38. Lyakhov, A. O. & Oganov, A. R. Evolutionary search for superhard materials: methodology and applications to forms of carbon and TiO_2. *Phys. Rev. B* **84**, 092103 (2011).
39. Zeng, K. Y. *et al*. Investigation of mechanical properties of transparent conducting oxide thin films. *Thin Solid Films* **443**, 60–65 (2003).
40. Perdew, J. P., Burke, K. & Ernzerhof, M. Generalized gradient approximation made simple. *Phys. Rev. Lett.* **77**, 3865–3868 (1996).
41. Heyd, J., Scuseria, G. E. & Ernzerhof, M. Hybrid functionals based on a screened *Coulomb* potential. *J. Chem. Phys.* **118**, 8207–8215 (2003).
42. Asahi, R. *et al*. Electronic and optical properties of anatase TiO_2. *Phys. Rev. B* **61**, 7459–7465 (2000).
43. Madsen, G. K. H. & Singh, D. J. BoltzTraP. A code for calculating band-structure dependent quantities. *Comput. Phys. Commun.* **175**, 67–71 (2006).
44. Jiang, X. *et al.* Aluminum-doped *Zinc oxide* films as transparent conductive electrode for organic light-emitting devices. *Appl. Phys. Lett.* **83**, 1875–1877 (2003).
45. Ginley, D. S. & Bright, C. Transparent conducting oxides. *Mat. Res. Sci. Bull.* **25**, 15–18 (2000).
46. Coutts, T. J. *et al*. Search for improved transparent conducting oxides: A fundamental investigation of *CdO*, Cd_2SnO_4, and Zn_2SnO_4. *J. Vac. Sci. Technol. A* **18**, 2646–2660 (2000).
47. Dali, S. E., Jayachandran, M. & Chockalingam, M. J. New transparent electronic conductor, $MgIn_2O_4$ spinel. *J. Mater. Sci. Lett.* **18**, 915–917 (1999).
48. Edwards, D. D. *et al*. A new transparent conducting oxide in the Ga_2O_3-In_2O_3-SnO_2 system. *Appl. Phys. Lett.* **70**, 1706–1708 (1997).
49. Minami, T. *et al*. Highly transparent and conductive $Zn_2In_2O_5$ thin films prepared by *RF* magnetron sputtering. *Jpn. J. Appl. Phys.* **34**, L971–L974 (1995).
50. Omata, T. *et al*. New ultraviolet-transport electroconductive oxide, $ZnGa_2O_4$ spinel. *Appl. Phys. Lett.* **64**, 1077–1078 (1994).
51. Kresse, G. & Furthmuller, J. Efficiency of ab initio total energy calculations for metals and semiconductors using a plane-wave basis set. *Phys. Rev. B* **54**, 11169–11186 (1996).
52. Klimes, J., Bowler, D. R. & Michaelides, A. Van der Waals density functionals applied to solids. *Phys. Rev. B* **83**, 195131 (2011).
53. Alfè, D. PHON: A program to calculate phonons using the small displacement method. *Comput. Phys. Commun.* **180**, 2622–2633 (2009).
54. Gajdoš, M. *et al.* Linear optical properties in the projector-augmented wave methodology. *Phys. Rev. B* **73**, 045112 (2006).
55. Roundy, D. *et al.* Ideal shear strengths of fcc *Aluminum* and *Copper*. *Phys. Rev. Lett.* **82**, 2713–2716 (1999).

Acknowledgments

This work is financial supported by the Fundamental Research Funds for the Central Universities (N130405003, N11080001), National Natural Science Foundation of China (No. 51001025), Program for Changjiang Scholars and Innovative Research Team in University (No. IRT0713), and National High Technology Research and Development Program of China (Grant No. 2013AA031601). We authors sincerely thank Dr. Qiang Zhu at State University of New York at Stony Brook for helpful discussion.

Author contributions

X.M., D.L. and X.D. perform USPEX structure-searching; H.P. and X.W. calculate properties of Ti-C-O compounds. All authors contribute to data analysis. X.M., G.Q. and L.Z. write the manuscript with inputs from all authors. X.M. and G.Q. direct the project.

Additional information

Supplementary information accompanies this paper at http://www.nature.com/scientificreports

Competing financial interests: The authors declare no competing financial interests.

How to cite this article: Meng, X. *et al*. Novel stable hard transparent conductors in TiO_2-TiC system: Design materials from scratch. *Sci. Rep.* **4**, 7503; DOI:10.1038/srep07503 (2014).